Turbulent Kinetic Energy Evolution in the Near Field of a Rotating-Pipe Round Jet

Mullyadzhanov, R; Abdurakipov, S.; Hanjalic, Kemal

DOI
10.1007/978-3-319-63212-4_71

Publication date
2018

Document Version
Final published version

Published in
Direct and Large-Eddy Simulation X

Turbulent Kinetic Energy Evolution in the Near Field of a Rotating-Pipe Round Jet

R. Mullyadzhanov, S. Abdurakipov and K. Hanjalić

1 Introduction

Using Large-Eddy Simulations (LES) and Proper Orthogonal Decomposition (POD) we study a turbulent round swirling jet issuing from an axially rotating pipe at Reynolds number $Re_b = 5300$ based on the bulk velocity U_b and diameter D of the pipe flow. The Reynolds number is chosen to match the available Direct numerical simulations (DNS) database for a pipe flow. The rotation rate is defined by the swirl parameter $N = U_w/U_b$ varying from 0 to 0.75 where U_w is the azimuthal velocity of the inner wall of the pipe. The aim is to explore the physics of a swirling flow when the inflow conditions of the problem are well defined. The broad literature on the subject of swirling jets suggests that the incoming velocity profile and the level of turbulence strongly affect the dynamics of the flow. Thus, the most important feature is the way one produces the swirl (e.g. tangential swirlers, rotating honeycombs etc.). The majority of configurations give the case-dependent velocity profiles in experiments which are hard to reproduce in computational studies. Here we study a jet flow issuing from a long rotating pipe. Thus, the incoming velocity profile is well defined. The main emphasis of this work is on coherent structures depending on the swirl intensity. The study in many ways follows the spirit of [1] who studied similar configuration but for low Reynolds numbers (laminar inflow).

R. Mullyadzhanov (✉)
Institute of Thermophysics SB RAS, Novosibirsk, Russia
e-mail: rustammul@gmail.com

S. Abdurakipov
Novosibirsk State University, Novosibirsk, Russia
e-mail: s.s.abdurakipov@gmail.com

S. Abdurakipov · K. Hanjalić
Delft University of Technology, Delft, Netherlands
e-mail: khanjalic@gmail.com

D.G.E. Grigoriadis et al. (eds.), *Direct and Large-Eddy Simulation X*,
ERCOFTAC Series 24, https://doi.org/10.1007/978-3-319-63212-4_71

2 Computational Details and Results

We consider a fully turbulent canonical rotating-pipe jet configuration (see Fig. 1, [2, 3]). The flow from a long clockwise-rotating pipe with the Reynolds number of 5300 is represented with a $1D$ pipe fragment. The total computational domain represents a cylinder of $12D$ in diameter and $16D$ in length. The convective outflow is imposed at the exit boundary, while constant pressure is imposed on the open lateral boundary. A small co-flow of $U_{co} = 0.04U_b$ is imposed at the bottom $x = -1D$. The LES grid has a DNS-like resolution in the near-nozzle area and consists of $252 \times 282 \times 264$ cells ($\sim 16.7 \times 10^6$) in the radial, axial, and azimuthal directions, respectively, with the majority clustered in shear layers and near-wall regions with the stretching factor being less than 5 percent. The minimum axial spacing $x = 0.005D$ is at the nozzle exit. Figure 1 also shows the mean axial and tangential pipe velocity profiles used at the inflow. Axial velocity displays some dependence on N and tendency to laminarization with higher N, while tangential velocity normalized with bulk velocity and N is almost insensitive to the rotation rate in this range.

The LES is performed using the TU Delft unstructured finite-volume computational code T-FlowS. The filtered Navier-Stokes and continuity equations for incompressible fluid are closed by the dynamic Smagorinsky subgrid-scale model. The diffusion and convection terms in the momentum equations are discretised by the second-order central-difference scheme, whereas the time-marching is performed using a fully-implicit three-level time scheme.

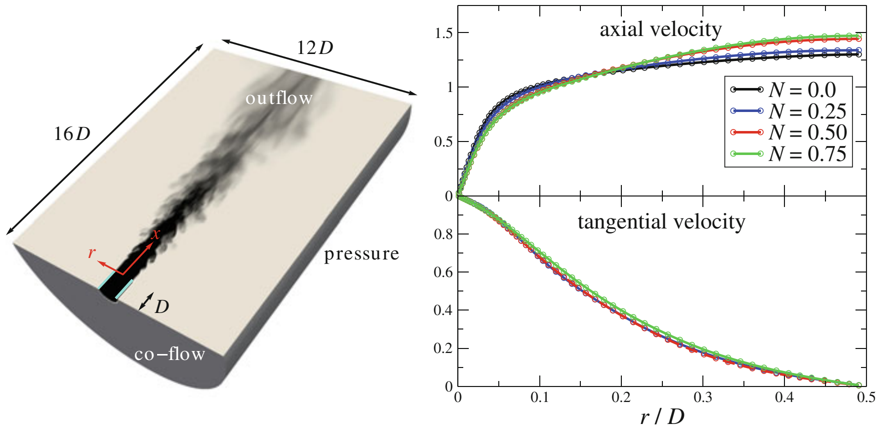

Fig. 1 *Left*: Half of the computational domain, cylindrical coordinate system (r, ϕ, x) and time-averaged axial and tangential velocity profiles from precursor LES of a periodic fully-developed turbulent pipe flow used as boundary conditions. The instantaneous field of a passive scalar is visualised. Cyan lines show the walls of the rotating pipe fragment. *Right*: Mean axial and tangential inflow pipe velocity profiles normalized with bulk velocity (tangential velocity is also normalized with N)

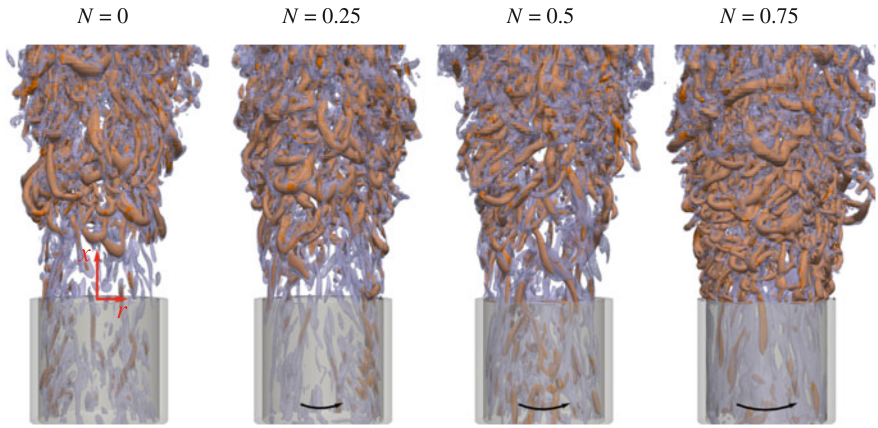

Fig. 2 The visualization of vortical structures near the nozzle of the jet using two isosurfaces of the Q-criterium with $Q = 0.5$ (*transparent violet*) and $Q = 1.5$ (*orange*) for various rotation rates. Black arrows show the clockwise rotation direction of the inner wall of the pipe

Figure 2 shows vortex structures in the near field of the jet. Vortices are visualized by constant levels of the Q-criterium where $Q = (\Omega_{ij}\Omega_{ij} - S_{ij}S_{ij})/2$ with Ω_{ij} and S_{ij} being the rotation rate and the rate-of-strain tensors, respectively. The pipe flow supplies the streamwise streaky structures which can be traced in the range of $0 \leq x/D \leq 1$. For $N = 0$ the interaction of streaky structures and the shear layer of the jet leads to the formation of the large-scale harpin-like structures at $x/D > 0.5$. Harpins are slightly tilted for low rotations $N = 0.25$ and can hardly be recognized for higher swirl. For relatively high rotation rates ($N = 0.75$) structures existing in the pipe are immediately destroyed by a strong azimuthal shear layer in the vicinity of the nozzle edge.

We perform Fourier decomposition with respect to ϕ and POD at various axial stations of the jet flow to get the information on the evolution of the amplitude and spatial distribution of modes corresponding to each azimuthal wavenumber m. We consider 32 stations starting from $x/D = 0$ with the last position at $x/D = 10$. The spatial step close to the nozzle is $\Delta x/D = 0.25$ while in the end it is fixed to $\Delta x/D = 0.5$. While most of low harmonics $|m| \leq 7$ grow with x along all of the distance, high m reach their saturation at $x/D = 1 - 2$ (not shown here). For $N = 0$ the axisymmetric mode $m = 0$ after exponential growth at $x/D < 1$ displays only some mild variations with x having the smallest λ among $|m| \leq 6$. Along $0 \leq x/D \leq 10$, there is a competition between the eigenvalues for different m. We can say that $m = 1, 2, 3$ contain the most of the turbulent kinetic energy, although, probably all low modes $|m| \leq 7$ have to be taken into account to reflect the dynamics correctly. At the same time, each high harmonic contains the more energy, the smaller the value of m. The higher the value of N, the stronger is the separation of $m = 1 - 3$ and other modes.

Further we analyze the motion from separate azimuthal modes m. It is convenient to operate in terms of propagating helical waves appearing as normal modes of the form $e^{i(m\phi+k_x x-\omega t)}$, where k_x is the streamwise wavenumber and ω is the frequency. In [4] they found the presence of single and double helix vortices which were supposed to correspond to $m = 1$ and 2 in the far field of a non-swirling jet. Note that the information obtained from a time sequence of two-dimensional slices of instanteneous velocity contains the mixture of co-rotating and counter-rotating modes with opposite m values (see, for example, the Conclusions in [5]). To be able to separate these helical patterns rotating in opposite directions, one may apply Fourier transform with two variable x and ϕ. However, the Fourier transorm requires periodic direction along the corresponding spatial variable. While possible, for example, for the infinite pipe flow, the Fourier transorm is not applicable to jets due to a significant radial expansion and evolution downstream. Recently, there was a successful attempt to statistically describe the flapping against helical motion of the jet core based on the information about the temporal amplitudes from POD [6].

Following [6], we analyze the temporal behaviour of a corresponding POD mode. We exclusively deal with temporal amplitudes a_q^m, where q is the number of a POD mode. Since they are complex-valued, the following representation is possible:

$$a(t) = \eta(t)e^{2\pi i\gamma(t)}, \tag{1}$$

where η and γ are the time sequences of real numbers. It was previously shown [6] that particular combinations of η and γ correspond to helical and flapping motion. The ideal helical motion represents a rotation of the jet core with constant angular velocity at some distance from the axis. Thus, one expects η to be constant and γ linearly grow in time. In terms of two azimuthal modes with opposite m values it means that one is present while the other cancels out. For the flapping motion both modes are present with the same rotation speed but opposite directions. This results in a more compicated behaviour of η and γ.

Figure 3 shows the behaviour of γ during 150 time units for first four q, m and $N = 0$; 0.5. A striking feature of $\gamma(t)$ is that it contains very long time intervals where it varies linearly. As pointed out above, it means that the corresponding spatial mode rotates around the jet core with some precession frequency. Dashed lines demonstrate the slope for some characteristic regions. This slope is in fact the non-dimensional angular velocity Ω. For example, three typical regions are shown in Fig. 3 (left) for $m = 1$: $\Omega \approx -0.87$; -0.21; 0.076. For $\Omega \approx -0.21$ and $\gamma = \Omega t$ the corresponding POD mode turns around in about 5 time units according to Eq. (1). These curves of $\gamma(t)$ for $m = 1$ demonstrate some intermittency showing changes of rotation direction within short time intervals (say, $t < 25$ with the typical value of $t = 5 - 10$), while in a long run the average rotation is non-zero. For higher m the behaviour is more monotonic, with the maximum absolute values $\Omega \approx -0.167$ for $m = 2$ and $\Omega \approx 0.08$ for $m = 3$. Similar trends can be found for $N = 0.5$.

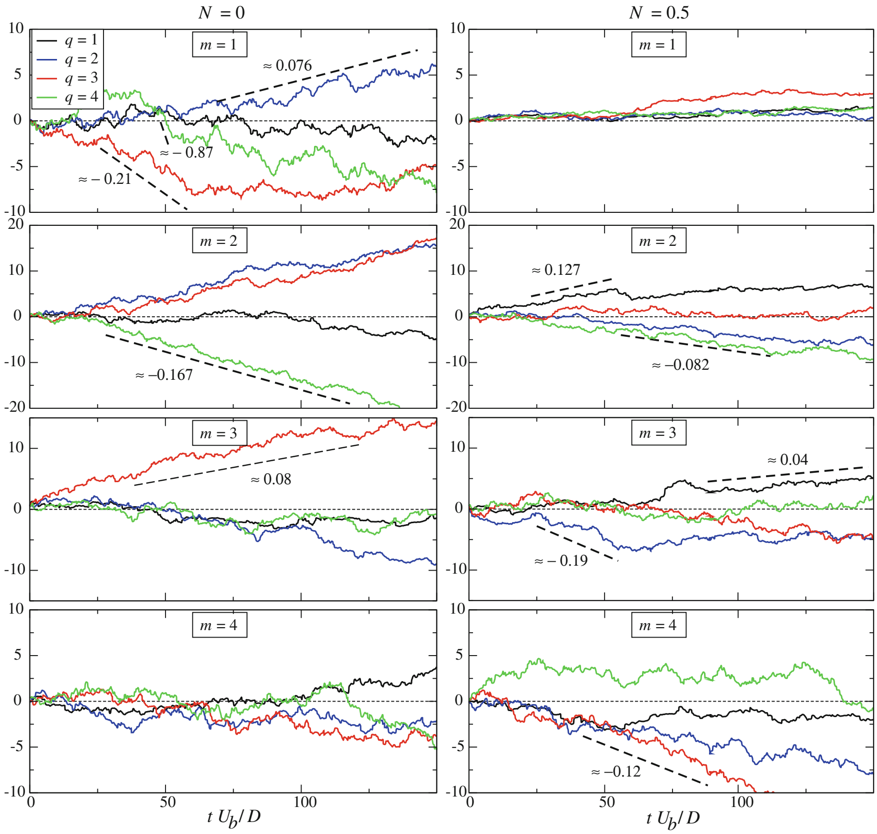

Fig. 3 The time history of the phase γ for different m and q (POD modes) for $x/D = 6$

3 Conclusions

We performed LES and POD analysis to get an insight into the coherent motion of the near nozzle area in a canonical rotating-pipe jet at $Re = 5300$ and $N = 0; 0.25; 0.5; 0.75$. We may conclude the following:

- The near-wall streaky structures identified by POD in a pipe flow can be recognised only along the first diameter of the pipe ($x/D < 1$) for low rotations $N \leq 0.5$. The azimuthal shear layer for a higher swirl ($N = 0.75$) immediately destroys pipe structures. Harpin-like vortices observed for a non-swirling jet as the interation of streaks and the shear layer are tilted at low rotation rates ($N = 0.25$) and cannot be recognized for higher swirl numbers.
- A set of low harmonics with the azimuthal numbers $|m| \leq 7$ are needed to describe the dynamics of the jet; the kinetic energy of high wavenumbers does not grow downstream. The kinetic energy for separate m grows linearly dowstream for first

$x = 5 - 8D$. The higher the rotation rate, the more obvious is the separation of energy between $m = 1 - 3$ modes and others.

- The phase of complex-valued POD temporal amplitudes $a(t)$ informs on the rotation dynamics of the corresponding mode around the axis of the jet. Low wavenumbers show two types of dynamics: "fast" and "slow" rotation. They differ in characteristic time scales of the process with $t < 25$ ($t = 5 - 10$) for the former and with up to $t = 150$ (or more) for the latter.

The described findings imply some important conclusions. As opposed to the periodic pipe flow where Fourier modes in axial and tangential directions are imposed by symmetries and represent basis functions in the form of propagating helical waves, the jet flow is inhomogeneous in axial direction restricting that class of functions. However, it is still possible to show that propagating helices are, indeed, the common form of POD modes for low azimuthal wavenumbers. Finally, it is interesting that the swirl does not ruin the helical structure of the jet. Probably it is due to the fast decay of the azimuthal velocity downstream. Indeed, it is known that the decay rate of the axial velocity in the far field of the jet is mainly governed by the axial momentum conservation law leading to a x^{-1} dependence. At the same time the conservation of angular momentum suggests the x^{-2} decay rate for azimuthal velocity. The same dependence is valid in the far field for the deviations of the axial velocity from the x^{-1} law if the jet nozzle is non-circular (see [7]). Thus, the conclusions made above on the dynamical structure may cover a wide range of free swirling non-circular turbulent jets which is to prove in following studies.

Acknowledgements This work is funded by Russian Science Foundation grant No. 14-19-01685. The computational resources are provided by Siberian Supercomputer Center SB RAS (Novosibirsk) and Joint Supercomputer Center RAS (Moscow).

References

1. Liang, H., Maxworthy, T.: An experimental investigation of swirling jets. J. Fluid Mech. **525**, 115–159 (2005)
2. Mullyadzhanov, R., Abdurakipov, S., Hanjalic, K.: Helical structures in the near field of a turbulent pipe jet. Flow Turbul. Combust. **98**(2), 367–388 (2017)
3. Mullyadzhanov, R., Abdurakipov, S., Hanjalic, K.: On coherent structures and mixing characteristics in the near field of a rotating-pipe jet. Int. J. Heat Fluid Flow **63**, 139–148 (2017)
4. Tso, J., Hussain, F.: Organized motions in a fully developed turbulent axisymmetric jet. J. Fluid Mech. **203**, 425–448 (1989)
5. Yoda, M., Hesselink, L., Mungal, M.G.: Instantaneous three-dimensional concentration measurements in the self-similar region of a round high-Schmidt-number jet. J. Fluid Mech. **279**, 313–350 (1994)
6. Davoust, S., Jacquin, L., Leclaire, B.: Dynamics of $m = 0$ and $m = 1$ modes and of streamwise vortices in a turbulent axisymmetric mixing layer. J. Fluid Mech. **709**, 408–444 (2012)
7. Mullyadzhanov, R.I., Yavorskii, N.I.: Solution of the problem of flow of a non-axisymmetric swirling submerged jet. J. Appl. Mech. Tech. Phys. **54**(2), 207–211 (2013)